Molecular Crystals and Liquid Crystals Science and Technology. Section A. Molecular Crystals and Liquid Crystals

Publication details, including instructions for authors and subscription information:
http://www.tandfonline.com/loi/gmcl19

Solitary Waves in an Antiferroelectric Liquid Crystal

Jian-Feng Li [a] , X. Y. Wang [a] , E. Kangas [a] , P. L. Taylor [a] , Charles Rosenblatt [a] , Yoshi-Ichi Suzuki [b] & P. E. Cladis [c]

[a] Department of Physics, Case Western Reserve University, Cleveland, Ohio, 44106, USA

[b] Central R&D Laboratory, Showa Shell Sekiyu Kabushiki Kaishi, Kanagawaken, JAPAN

[c] AT&T Bell Laboratories, Murray Hill, N.J., 07974, USA

Version of record first published: 24 Sep 2006.

To cite this article: Jian-Feng Li , X. Y. Wang , E. Kangas , P. L. Taylor , Charles Rosenblatt , Yoshi-Ichi Suzuki & P. E. Cladis (1996): Solitary Waves in an Antiferroelectric Liquid Crystal, Molecular Crystals and Liquid Crystals Science and Technology. Section A. Molecular Crystals and Liquid Crystals, 288:1, 73-82

To link to this article: http://dx.doi.org/10.1080/10587259608034585

Mol. Cryst. Liq. Cryst., 1996, Vol. 288, pp. 73–82
Reprints available directly from the publisher
Photocopying permitted by license only

SOLITARY WAVES IN AN ANTIFERROELECTRIC LIQUID CRYSTAL

JIAN-FENG LI[†], X.Y.WANG[†], E.KANGAS[†], P.L.TAYLOR[†], CHARLES ROSENBLATT[†], YOSHI-ICHI SUZUKI[‡] AND P.E.CLADIS[#]
[†]Department of Physics, Case Western Reserve University, Cleveland, Ohio 44106, USA, [‡]Central R&D Laboratory, Showa Shell Sekiyu Kabushiki Kaishi, Kanagawaken, JAPAN, [#]AT&T Bell Laboratories, Murray Hill, N.J. 07974, USA

Abstract The antiferroelectric liquid crystalline phase and related ferrielectric phases exhibit a rich variety of physical behavior. Recently we have been examining the dynamics of these materials. For materials whose dielectric anisotropy $\Delta\varepsilon < 0$, we find a critical threshold d.c. field E_{th} in the Sm C_A* phase, above which solitary waves propagate rapidly along the layer direction. These solitary waves, which consist of ferroelectric regions propogating into an antiferroelectric sea, may be "frozen" in place by reducing the field to E_{th}, or forced to retreat by reducing the field to $E < E_{th}$.

Antiferroelectric liquid crystals (AFLCs) have presented many new and exciting challenges[1,2,3]. AFLCs exhibit a layered structure in which the molecules are tilted in one layer by an angle θ relative to the layer normal and by $-\theta$ in the adjacent layers, with no long range positional order within the layer plane (see Fig. 1). For each smectic layer there is an associated polarization.

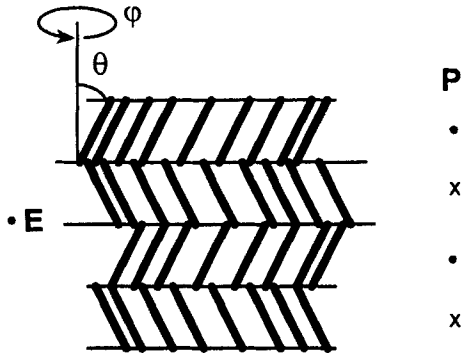

FIGURE 1 Schematic representation of surface stabilized antiferroelectric state.

$\vec{P}_o$ which lies in the plane of the layer and perpendicular to the molecules; in neighboring layers the polarization vectors are *nearly* antiparallel owing to a long-pitch helical structure. In a sufficiently large applied electric field the helix unwinds, giving rise to field-induced long-range ferroelectric ordering[4] characterized by a saturated net polarization and a molecular tilt θ relative to the layer normal. Ferrielectric states, which we define such that adjacent layers are no longer required to have opposite polarizations, connect the P = 0 antiferroelectric state to the fully saturated polarization of the ferroelectric state.

In AFLCs it has been observed that the transition from the highest-field ferrielectric state to a ferroelectric state is characterized by ferroelectric fingers propagating into the ferrielectric region[5], even at frequencies of 1 kHz. Here we show that the AFLC ferrielectric - ferroelectric transition at f = 0 is characterized by a threshold field E_{th} that is independent of sample thickness. Moreover, we show that the propagation speed $v = v_o(E - E_{th})/E_{th}$ for $|(E - E_{th})/E_{th}| \ll 1$, where v_o is material-dependent and is typically a few centimeters per second[6]. Finally, we observe that the fingering is reversible when E is reduced below E_{th}. We model these results with an elastic energy that includes chiral, dielectric, and surface effects and, importantly, an

interlayer coupling[7]. In this model the dynamics are driven by dielectric effects and the interlayer coupling determines E_{th}. These features account for the independence of E_{th} on sample thickness.

Cells were constructed of electrically-conducting indium-tin-oxide coated glass plates, which were first dipped in a solution of nylon 6/6 in formic acid and allowed to drip dry. The slides were then rubbed unidirectionally, placed together (with the rubbing directions parallel) separated by a pair of mylar spacers of thickness *d*, and cemented. The cell spacings *d* varied from 2 μm to 14 μm. The cells were filled with the liquid crystal TFMHPOBC [4-(1-trifluoromethylhexyloxycarbonyl) phenyl 4'-octyloxybiphenyl-4-carboxylate, Ref. 8] in the isotropic phase, placed into a temperature controlled oven, and allowed to cool into the antiferroelectric Sm C_A* phase. The temperature was stabilized at (110.00 ± 0.01) °C, *i.e.* ~3.5 °C below the smectic A - antiferroelectric smectic C_A* transition, and the sample was viewed through a polarizing optical microscope; a texture-free, planar orientation was observed. A d.c. electric field was then applied to the sample. For sufficiently small field no obvious change in the appearance of the sample was observed; above a threshold field E_{th} however, bright fingers, which expand in the plane of the layers and are of width several micrometers, began to appear under the crossed polarizers. The appearance of fingers occurred at a characteristic threshold *field*, independent of *d* to within experimental uncertainty (Table 1).

TABLE 1 Experimental parameters

Spacer Thickness (μm)	**E_{th} (statv cm^{-1})**	**v_0 (cm s^{-1})**
5 ± 1 (Nylon)	242 ± 40	2.9 ± 0.4 (Advancing) -2.6 ± 0.5 (Retreating)
9 ± 1 (Nylon)	260 ± 35	3.1 ± 0.4 (Advancing)
12.5 ± 1 (Nylon)	227 ± 35	2.6 ± 0.4 (Advancing) -4.5 ± 0.5 (Retreating)
14 ± 1 (Polyimide)	263 ± 35	4.5 ± 0.5 (Advancing) -4.3 ± 0.5 (Retreating)

To measure v *vs.* E a square wave of period 8 s was applied to the sample. The image was recorded using a CCD camera and videocassette recorder, with an overall spatial resolution of approximately 2 μm. The recording was played back frame-by-frame with temporal resolution of 0.0167 s. The position of the propagating tip of the finger was measured on the screen, thereby yielding the velocity *vs.* E. In Fig. 2 we show v *vs.* positive reduced field $(E - E_{th}) / E_{th}$ for three different cell spacings [5 μm (triangle),

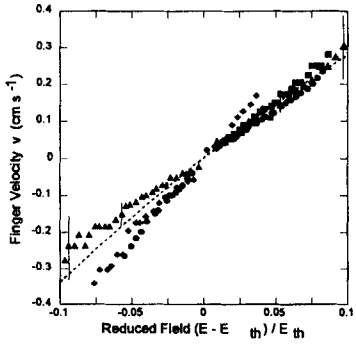

FIGURE 2 Experimental velocity *vs.* reduced field. See text for cell thicknesses and surface treatment of each data set. Dashed line respresents model calculation using $P_0 = 225$ esu cm^{-2}, $2U = 5.6 \times 10^4$ erg cm^{-3}, $\gamma = 0.25$ P, $\Delta\varepsilon = -1.1$, and $K = 1 \times 10^{-6}$ dyn

9 μm (square), and 12.5 μm (circle)] with nylon-treated surfaces; these correspond to advancing fingers. We also show retreating fingers for $E < E_{th}$ for the 5 μm (triangle) and 12.5 μm (circle) cells. Values for E_{th} are given in Table 1. The effects of surface treatment are shown in Fig. 2 for a polyimide aligning agent with cell thickness d = 14 μm (diamond); both advancing and retreating fingers are shown. In this plot $v_0 = (4.5 \pm 0.5)$ cm s^{-1}, while for most of the nylon surfaces (except for the retreating 12.5 μm cell) $v_0 \sim (2.9 \pm 0.4)$ cm s^{-1}; we do not have an explanation for this one

counterexample. We believe that the width of the propagating fingers is closely related to the pitch of the bulk antiferroelectric phase, as a fraction of the pitch corresponds to a characteristic distance over which the azimuthal orientations are in register.

The modeling of nonlinear finger propagation has been an active field of study[7,9,10,11,12,13,14,15,16,17,18]. To model our observed behavior, we consider the picture in Fig. 3.

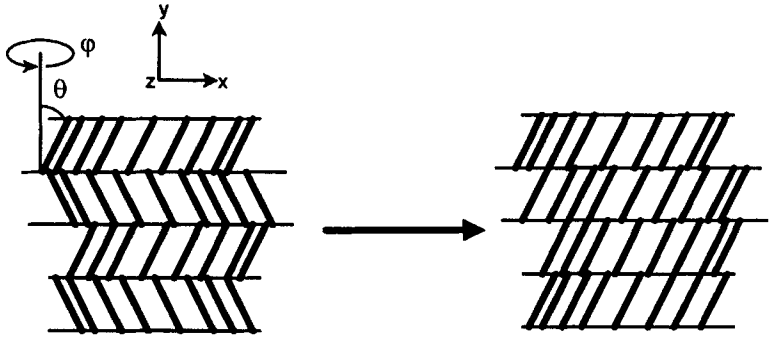

FIGURE 3 Schematic representation of field-induced ferroelectric ordering

We start with the free energy for an unwound helix proposed by Wang and Taylor [7]. The free energy $F = \sum_i \int f_i dx$, where $f_i = f_i^{elastic} + f_i^{electric} + f_i^{layer-layer} + f_i^{surface} + f_i^{chiral}$:

$$f_i = \frac{1}{2} K \sin^2\theta \left[\left(\frac{\partial \varphi_i}{\partial x}\right)^2 + \left(\frac{\partial \varphi_i}{\partial z}\right)^2 \right] - P_o E \cos\varphi_i - \left(\frac{\Delta\varepsilon \sin^2\theta}{8\pi} E^2 - W(z) \right) \sin^2\varphi_i$$

$$- b \sin(\varphi_{i-1} - \varphi_i) + \frac{U}{2} \left[\cos(\varphi_{i-1} - \varphi_i) + \cos(\varphi_i - \varphi_{i+1}) \right] \qquad (1)$$

Here f_i is the free energy density of the i^{th} smectic layer; $K \sin^2\theta$ is the effective elastic constant associated with a change in azimuthal orientation φ along the $\hat{x}$ – axis (within a smectic layer); P_o is the local polarization; b is a term associated with chirality; W(z) is the anchoring strength at the interfaces, *viz.*, $W(z) = w_o [\delta(z-½d)+ \delta(z+½d)]$; and $\Delta\varepsilon$

is the dielectric anisotropy. The coupling between layers is expressed in terms of the coupling coefficient U, which has dimensions of energy per volume, and represents a local interaction involving dipoles and possibly steric effects. It is the presence of the chiral, surface, and interaction (U) terms that distinguishes the present model from previously extant models, such that the interaction term in particular introduces new physical phenomena.

We now take the equations of motion found from Eq. 1 and introduce a viscosity γ associated with azimuthal rotations of the director. The basic physics may be gleaned by neglecting the chiral term b and anchoring term W, which we shall do in the interest of simplifying the calculations. In the overdamped limit we find for $i = 1, 2, 3, ..., n$:

$$\gamma \frac{\partial \varphi_i}{\partial t} = K \sin^2\theta \frac{\partial^2 \varphi_i}{\partial x^2} - P_o E \sin\varphi_i + \frac{\Delta\varepsilon \sin^2\theta}{8\pi} E^2 \sin 2\varphi_i - U\left[\sin(\varphi_{i-1} - \varphi_i) - \sin(\varphi_i - \varphi_{i+1})\right] \quad (2)$$

In the antiferroelectric state the total polarization vanishes when E = 0. We assume the simplest model for this situation, *viz.*, a herringbone structure in which alternate layers have $\varphi = 0$ and $\varphi = \pi$ when the helical structure is suppressed[19]. Those layers with $\varphi = 0$ will be unaffected by the applied field, but those with $\varphi = \pi$ will become unstable at sufficiently large fields. We accordingly make the approximation of putting $\varphi_i = 0$ for all odd i and $\varphi_i = \varphi$ for even i. Eq. 2 then reduces to the single equation

$$\gamma \frac{\partial \varphi}{\partial t} - K \sin^2\theta \frac{\partial^2 \varphi}{\partial x^2} = (2U - P_o E)\sin\varphi + \frac{\Delta\varepsilon \sin^2\theta}{8\pi} E^2 \sin 2\varphi \equiv g(\varphi), \quad (3)$$

where $\varphi \equiv \varphi_2$. An exact solitary-wave solution to Eq. 3 is [Ref.9-11]

$$\varphi = 2\tan^{-1}\left\{exp\left[\sqrt{\frac{-\Delta\varepsilon}{\pi K}}\frac{E}{2}(x - vt)\right]\right\}. \tag{4}$$

For this solution to be physically valid $\Delta\varepsilon$ must be negative[11]. It has been shown to be stable in the limited range of E for which $g'(\varphi)\big|_{\varphi=0} < 0$ when $0 < E < E_{th}$ and $g'(\varphi)\big|_{\varphi=\pi} < 0$ when $E > E_{th}$ [Ref. 9]. The velocity v is given by

$$v = \left(\frac{P_o - \frac{2U}{E}}{\gamma}\right)\frac{2\sqrt{\pi K}}{\sqrt{-\Delta\varepsilon}} \equiv v_o\frac{E - E_{th}}{E}, \tag{5}$$

with $E_{th} = \frac{2U}{P_o}$ and [Ref. 20]

$$v_o = \frac{2P_o\sqrt{\pi K}}{\gamma\sqrt{-\Delta\varepsilon}}. \tag{6}$$

Physically, this solution corresponds to a region of ferroelectricity (for which $\varphi = 0$ in *all* layers) propagating into or retreating from the antiferroelectric region with velocity v, as shown in Fig. 4. The finger "tip" has a width given by $\xi = \frac{2}{E}\sqrt{-\frac{\pi K}{\Delta\varepsilon}}$, for $\Delta\varepsilon < 0$, and is typically a few thousand Å.

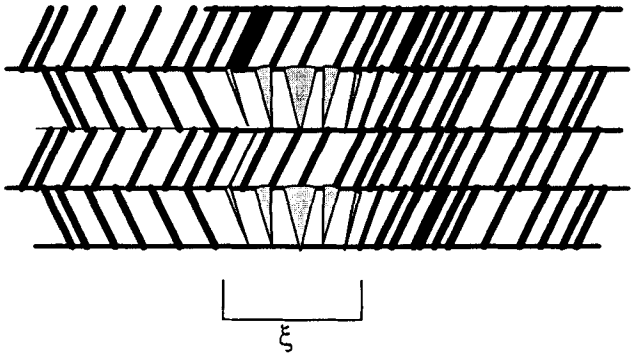

FIGURE 4 Schematic representation of ferroelectric region propagating into the antiferroelectric region (from right to left). The region ξ corresponds to the width of the finger "tip."

Taking the literature value $P_o \sim 225$ esu cm^{-2} [Ref. 8], we find that for a typical measured threshold field of $E_{th} \sim 250$ statv cm^{-1}, the quantity 2U is approximately 5.6 x 10^4 erg cm^{-3}, or approximately P_o^2; this indicates strong interlayer coupling. We can also examine the velocity profile using Eq. 5. Using a homeotropically-aligned and a planar-aligned sample, we measured $\Delta\varepsilon = -1.1 \pm 0.1$. The velocity data in Fig. 3 is then well described by Eq. 5 if we assume that $\sqrt{K} / \gamma \sim 4 \times 10^{-3}$ cgs. The calculated velocity for these parameters is shown by a solid line in Fig. 3. Since $K \sim 10^{-6}$ dyn, our data yields a viscosity $\gamma \sim 0.25$ poise, a value typical for liquid crystals. In addition, we note that the experiment was performed at fields close to E_{th} where v can be approximated by $v_o[(E - E_{th}) / E_{th}]$. We find from the model that $v_o \sim 3.0$ cm s^{-1}, consistent with the experimental values given in Table 1. For $E < E_{th}$ both theory and experiment show that the solitary wave propagates with a negative velocity as the ferrielectric phase is recovered.

If account is taken of surface anchoring, the velocity v_o is given approximately by

$$v_o \approx \frac{2P_o\sqrt{\pi K}}{\gamma\sqrt{-\Delta\varepsilon}}\left(1+\frac{8\pi w_o}{d\Delta\varepsilon E^2 \sin^2\theta}\right). \quad (7)$$

Thus, the velocity is expected to decrease with increasing anchoring strength and decreasing sample thickness. As Table 1 indicates that thickness plays little role, we believe that anchoring — at least for the samples we've studied — is not important.

If the field is suddenly switched off, we experimentally find that the antiferroelectric phase recovers with a velocity much faster than we can determine with our current apparatus. If the mechanism for this ultrafast recovery of the antiferroelectric phase were solitary-wave propagation, heretofore unobserved in other liquid crystal systems for small fields, then we might expect its velocity to be given by the solution of Eq. 3 with E = 0. Aronson and Weinberger[13] have rigorously shown this to be $v = v_o\sqrt{-2U\Delta\varepsilon \sin^2\theta / \pi P_o^2}$. To determine the tilt angle θ we observed a planar-aligned sample through a polarizing microscope. The stage of the microscope was rotated to obtain extinction of transmitted light in the presence of large positive and negative d.c. fields, and θ was found to be $(20 \pm 1)^o$. The velocity v would then be of order 1 cm s^{-1}. Future measurements at higher propagation speeds, fields, and varying temperatures should indicate whether the ferroelectric to antiferroelectric mechanism is front propagation or of some other character, such as bulk relaxation[11,16].

Acknowledgements: This work was supported by the National Science Foundation's Solid State Chemistry program under grant DMR-9502925, and by the Donors of the Petroleum Research Fund, administered by the American Chemical Society.

REFERENCES

1. A.D.L. Chandani, T. Hagiwara, Y. Suzuki, Y. Ouchi, H. Takezoe, and A. Fukuda, Jpn. J. Appl. Phys. **27**, L729 (1988)
2. see A. Fukuda, Y. Takanishi, T. Isozaki, K. Ishikawa, and H. Takezoe, J. Mater. Chem. **4**, 997 (1994)
3. Y. Yamada, N. Yamamoto, K. Mori, K. Nakamura, T. Hagiwara, Y. Suzuki, I. Kawamura, H. Orighara, and Y. Ishibashi, Jpn. J. Appl. Phys. **29**, 1757 (1990)
4. R.B. Meyer, L. Liebert, L. Strzelecki, and P. Keller, J. Physique Lett. **36**, L69 (1975)
5. P.E. Cladis and H.R. Brand, Liq. Cryst. **14**, 1327 (1993)
6. J.-F. Li, X.Y. Wang, E. Kangas, P.L. Taylor, C. Rosenblatt, Y. Suzuki, and P.E. Cladis, Phys. Rev. B **52**, R13075 (1995)
7. X.Y. Wang and P.L. Taylor, Phys. Rev. Lett. (in press)
8. Y. Suzuki, H. Hagiwara, I. Kawamura, N. Okamura, T. Kitazume, M. Kakimoto, Y. Imai, Y. Ouchi, H. Takezoe, and A. Fukuda, Liq. Cryst. **6**, 167 (1989)
9. E. Magyari, Phys. Rev. B **29**, 7082 (1984).
10. D.K. Campbell, M. Peyrard, and P. Sodano, Physica **19D**, 204 (1986)
11. P.E. Cladis and W. van Saarloos in **Solitons in Liquid Crystals**, ed. by L. Lam and J. Prost, (Springer-Verlag, New Yorkn 1992).
12. X.Y. Wang, Phys. Rev. A **32**, 3126 (1985)
13. D.G. Aronson and H.F. Weinberger, **Partial Differential Equations and Related Topics**, ed. by J. Goldstein, (Springer-Verlag, 1975; Adv. Math. **30**, 33 (1978)
14. G. Dee and J.S. Langer, Phys. Rev. Lett. **50**, 383 (1983)
15. W. van Saarloos, Phys. Rev. A **39**, 6367 (1989)
16. P.E. Cladis, H.R. Brand, and P.L. Finn, Phys. Rev. A **28**, 512 (1983)
17. J.E. Maclennan, N.A. Clark, and M.A. Handschy in **Solitons in Liquid Crystals**, ed. by L. Lam and J. Prost, (Springer-Verlag, New York, 1992).
18. W. van Saarloos, M. van Hecke, and R. Holyst, Phys. Rev. E (in press)
19. Y. Galerne and L. Liebert, Phys. Rev. Lett. **66**, 2891 (1991)
20. Note that $v \begin{matrix} < \\ > \end{matrix} 0$ is determined by the condition $\int_0^{\pi} g(\varphi) d\varphi \begin{matrix} > \\ < \end{matrix} 0$.